Investigating tumour vascular connectivity with resting state MRI and independent component analysis

Miguel R. Gonçalves[1,2], Simon Walker-Samuel[1], Sean P. Johnson[2], Rosamund B. Pedley[2], and Mark F. Lythgoe[1]

[1]UCL Centre for Advanced Biomedical Imaging, Division of Medicine and Institute of Child Health, University College London, London, United Kingdom, [2]UCL Cancer Institute, London, United Kingdom

Introduction: Solid tumours have been observed to exhibit regions of transient, cycling hypoxia and subsequent reoxygenation due to spontaneous fluctuations in blood flow and oxygenation [1, 2]. This has been shown to contribute to resistance to chemotherapy [3] and radiotherapy [4], as well as tumour progression and development of metastatic disease [5, 6]. It has also been observed that spontaneous fluctuations in tumour oxygenation are spatially correlated with functionally perfused regions [1, 7]. Independent component analysis (ICA) [8] has been used in the brain to identify resting state network patterns of activation [9]. It allows for the detection of coherent oscillations in blood flow and oxygenation by decomposing the data into a number of independent components (ICs). Given the conceptual similarity between tumour fluctuations and that of coherent haemodynamic oscillations in the brain, we considered the use of ICA to study transient, cyclical events, in order to characterise tumour vascular connectivity and identify regions with common pathophysiology.

Methods: $5x10^6$ SW1222 (n=4) or LS174T (n=3) colorectal carcinoma (CRC) cells were injected subcutaneously into MF1 *nu/nu* mice (week 0). After tumours had grown to an approximate volume of $1cm^3$ (weeks 2-3), tumours were imaged using a 9.4T Agilent VNMRS 20 cm horizontal-bore system, with a 39 mm birdcage coil, using a multi-slice, multi-gradient echo (GEMS) sequence. Mice were anaesthetised using isoflurane (1.25% in medical air). Respiratory frequency varied between 65-90 breaths/min and temperature was maintained at 36.7 °C. A 70min scan was performed to evaluate spontaneous fluctuations in tumour R_2* (=$1/T_2$*), with a temporal resolution of 16.8 seconds. This was followed by a series of gas challenges with air and carbogen (95% oxygen, 5% carbon dioxide) breathing whilst acquiring GEMS data with the same sequence. Voxel-wise post processing was performed in Matlab: i) **Resting state$_{(SD)}$** maps depict the standard deviation of R_2^* resting state (RS) time courses in each voxel. ii) **Resting state$_{(FFT)}$** plots were obtained by Fourier transforming R_2^* RS time courses, to display frequency patterns of oscillations. iii) **Resting State$_{(ICA)}$** maps were created from Principal Component Analysis (PCA) and further decomposition into independent components (ICs) with ICA [8]. After decomposition, the ICA spatial maps were z-transformed and colour-coded according to their absolute value and sign. iv) **Gas Challenge$_{(diff)}$** maps of vascular functionality were calculated from the difference between administration of carbogen and air [10]. *GEMS parameters: Spoiled gradient-echo (SPGR) sequence with TR=262.9440ms, 5 echoes TE_1=2ms, echo spacing=2ms, 22 slices, 64x64 matrix, voxel volume 350x350x500 microns, flip angle=20°.*

Results: We present maps of i) Resting State$_{(SD)}$, ii) Resting State$_{(FFT)}$, iii) Resting State$_{(ICA)}$ and iv) Gas Challenge$_{(diff)}$. Variations in R_2^* are clearly seen across the **Resting State$_{(SD)}$** maps (Figs. 1a and 2a). There are also marked differences between the resting states of SW1222 and LS174T tumours. No such variations were observed in normal muscle tissue (Fig. 3). **Resting State$_{(FFT)}$** showed dominant frequencies at <0.9 cycles/min for both tumour types (Figs. 1b and 2b) and as expected, similar patterns to the Resting State$_{(SD)}$. Higher frequency oscillations were also observed at 1.1 and 1.6 cycles/min. Furthermore, **Resting State$_{(ICA)}$** demonstrated regions of common coherent oscillatory patterns (1c and 2c), substantiated by clusters of similar z-score. A high (>2, white) or low (<-2, purple) z-score implies strong correspondence with a particular temporal pattern. Interestingly, Resting State$_{(ICA)}$ maps provided additional information over and above Resting State$_{(SD)}$ (Figs. 1a and 1c, arrows), as regions with opposing z-scores are identified as having anti-correlated temporal patterns, and thus may represent regions subject to intra-tumour vascular steal [11]. These clusters of connected pixels can extend through multiple slices within the tumours (Figs. 1d and 2d). Finally, using **Gas Challenge$_{(diff)}$** maps, we observed a decrease in R_2^* when switching from air breathing to carbogen breathing (blue voxels) indicating these regions were shown to be functionally perfused (Figs. 1e and 2e, arrows).

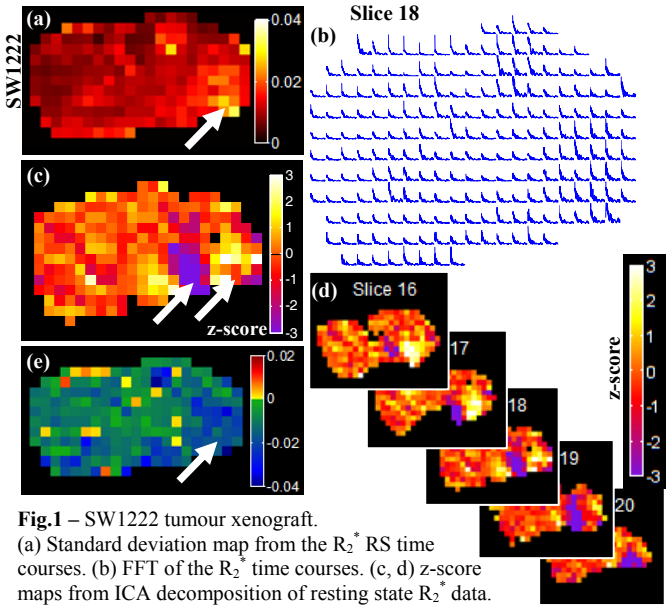

Fig.1 – SW1222 tumour xenograft. (a) Standard deviation map from the R_2^* RS time courses. (b) FFT of the R_2^* time courses. (c, d) z-score maps from ICA decomposition of resting state R_2^* data. One IC is shown. (e) Gas challenge breathing between carbogen and air.

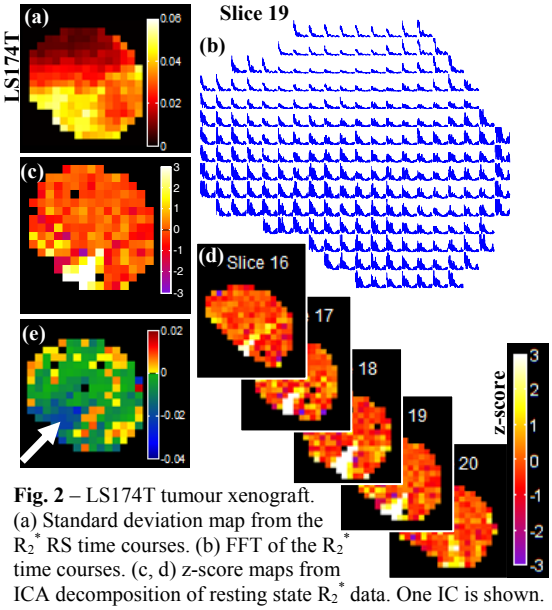

Fig. 2 – LS174T tumour xenograft. (a) Standard deviation map from the R_2^* RS time courses. (b) FFT of the R_2^* time courses. (c, d) z-score maps from ICA decomposition of resting state R_2^* data. One IC is shown. (e) Gas challenge breathing between carbogen and air.

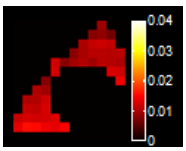

Fig. 3 – Standard deviation map of the R_2^* time-courses in muscle tissue. Note the low values in comparison with the tumours.

Discussion & Conclusion: ICA of resting state tumour data identified clusters of voxels with similar temporal characteristics suggesting regions of similar hemodynamic functionality, i.e., subject to correlated spontaneous fluctuations in blood flow. Clusters with opposite z-scores represent regions fluctuating with the same temporal pattern, but anti-correlated, possibly reflecting regions subject to intra-tumour vascular steal. Spontaneous fluctuations in tumour blood flow are thought to be caused by inefficient vascular networks and high interstitial fluid pressure evident in tumours, alongside systemic changes in blood pressure. This is the first reported application of ICA in this context, although further measurements are necessary to accurately identify the observed clustering effects. In conclusion, ICA may provide a powerful approach for differentiating between regions of tumour tissue with differing and/or connected vascular physiology, or to discriminate systemic variations from localised tumour effects.

Acknowledgements: This work was carried out as part of King's College London and UCL Comprehensive Cancer Imaging Centre CR-UK & EPSRC, in association with the MRC, DoH and British Heart Foundation (England).

References: [1] Baudelet C, *et al., Phys. Med. Biol.* 49: 3389-411. [2] Brown JM, *Br. J. Radiol.* 52: 650-6. [3] Durand RE, *Cancer and Metastasis Rev.* 20: 57-61. [4] Chaplin DJ, *et al., Cancer Res.* 47: 597-601. [5] Hill RP, *Cancer and metastasis Rev.* 9:137-47. [6] Cairns RA, *et al., Cancer Res.* 61:8903-8. [7] Gonçalves MR, *et al.* Poster presentation British Chapter ISMRM, Cambridge, 2011. [8] Hyvärinen A, *IEEE Trans. Neural Netw.* 10:626-34. [9] van de Ven, *et al., Hum. Brain Mapp.* 22: 165-78. [10] Baudelet C, *et al., NMR Biomed.* 19:69-76. [11] Dewhirst MW, *et al. Radiat Res.* 130:345-54.